Role of metal ions in the reaction catalyzed by L-ribulose-5-phosphate 4-epimerase.

ARTICLE *in* BIOCHEMISTRY · MAY 2000

Impact Factor: 3.02 · Source: PubMed

4 AUTHORS, INCLUDING:

Russell R Poyner
University of Wisconsin–Madison
21 PUBLICATIONS **521** CITATIONS

Role of Metal Ions in the Reaction Catalyzed by L-Ribulose-5-phosphate 4-Epimerase†

Lac V. Lee, Russell R. Poyner, Maria V. Vu, and W. W. Cleland*

Institute for Enzyme Research and Department of Biochemistry, University of Wisconsin, Madison, Wisconsin 53705

Received December 17, 1999

ABSTRACT: H97N, H95N, and Y229F mutants of L-ribulose-5-phosphate 4-epimerase had 10, 1, and 0.1%, respectively, of the activity of the wild-type (WT) enzyme when activated by Zn^{2+}, the physiological activator. Co^{2+} and Mn^{2+} replaced Zn^{2+} in Y229F and WT enzymes, although less effectively with the His mutants, while Mg^{2+} was a poorly bound, weak activator. None of the other eight tyrosines mutated to phenylalanine caused a major loss of activity. The near-UV CD spectra of all enzymes were nearly identical in the absence of metal ions and substrate, and addition of substrate without metal ion showed no effect. When both substrate and Zn^{2+} were present, however, the positive band at 266 nm increased while the negative one at 290 nm decreased in ellipticity. The changes for the WT and Y229F enzymes were greater than for the two His mutants. With Co^{2+} as the metal ion, the CD and absorption spectra in the visible region were different, showing little ellipticity in the absence of substrate and a weak absorption band at 508 nm. With substrate present, however, an intense absorption band at 555 nm ($\epsilon = 150-175$) with a negative molar ellipticity approaching 2000 deg cm^2 dmol^{-1} appears with WT and Y229F enzymes. With the His mutants, the changes induced by substrate were smaller, with negative ellipticity only half as great. The WT, Y229F, H95N, and H97N enzymes all catalyze a slow aldol condensation of dihydroxyacetone and glycolaldehyde phosphate with an initial k_{cat} of 1.6×10^{-3} s^{-1}. The initial rate slowed most rapidly with WT and H97N enzymes, which have the highest affinity for the ketopentose phosphates formed in the condensation. The EPR spectrum of enzyme with Mn^{2+} exhibited a drastic decrease upon substrate addition, and by using $H_2{}^{17}O$, it was determined that there were three waters in the coordination sphere of Mn^{2+} in the absence of substrate. These data suggest that (1) the substrate coordinates to the enzyme-bound metal ion, (2) His95 and His97 are likely metal ion ligands, and (3) Tyr229 is not a metal ion ligand, but may play another role in catalysis, possibly as an acid−base catalyst.

L-Ribulose-5-phosphate 4-epimerase (araD, EC 5.1.3.4) catalyzes the interconversion of L-ribulose 5-phosphate (L-Ru5P)[1] and D-xylulose 5-phosphate (D-Xu5P) by changing the stereochemistry at C-4 (*1*). In the previous paper (*2*), measurements of ^{13}C and deuterium kinetic isotope effects were employed to produce compelling evidence that the 4-epimerase catalyzes the epimerization reaction via an aldol cleavage−condensation mechanism. The focus of this work was to determine which divalent metal ion is preferred by the 4-epimerase for catalysis, the role of the requisite metal ion in the catalysis, and what the metal ion ligands are in the active site of the enzyme. To address these problems, we employed site-specific mutagenesis, steady-state kinetics, and spectroscopy.

EXPERIMENTAL PROCEDURES

Preparation of B(DE3)araD⁻ pLysS Escherichia coli. To generate mutant 4-epimerases that are free of the wild-type contamination, an *E. coli* host bearing the T7 RNA polymerase gene for expression of the target protein was needed but the host had to be incapable of generating the wild-type epimerase from its chromosome. To produce a wild-type deficient host, araD^{-139} *E. coli* strain B [a gift from N. Lee from the University of California at Santa Barbara, Santa Barbara, CA (*1*)] was lysogenized with λDE3 bacteriophage containing the T7 RNA polymerase gene. The procedure for the generation of the host *E. coli* was followed according to the instructions of the λDE3 Lysogenization Kit from Novagen.

The araD$^-$ cells were grown in LB medium supplemented with 0.2% maltose and 10 mM $MgSO_4$ to an OD_{600} of 0.5. Four microliters of the λDE3 phage lysate, 2.8 μL of the helper phage lysate, and 1.8 μL of the selection phage lysate were incubated with 1 μL of the araD$^-$ cells at 37 °C for 20 min. The mixture was then plated on an LB agar plate.

Verification of the lysogens using T7 tester phage was necessary to make certain that the desired colonies would be properly lysogenized by the prescribed method. Three colonies were taken from the agar plate for testing. Each was grown in LB medium with 0.2% maltose and 10 mM $MgSO_4$ to an OD_{600} of 0.5. The tester phage was diluted 10^6-fold, and 100 μL of the diluted tester phage was incubated with 100 μL of the lysogenized cells at 37 °C for 20 min. Half of each sample was plated onto three LB agar

† Supported by Grant GM 18938 from the National Institutes of Health. R.R.P. was supported by Grant GM 35752 from the National Institutes of Health.

* To whom correspondence should be addressed: 1710 University Ave., Madison, WI 53705. Phone: (608) 262-1373. Fax: (608) 265-2904. E-mail: cleland@enzyme.wisc.edu.

[1] Abbreviations: L-Ru5P, L-ribulose 5-phosphate; D-Xu5P, D-xylulose 5-phosphate; L-Fuc1P, L-fuculose 1-phosphate; L-Rhu1P, L-rhamnulose 1-phosphate; IRMS, isotope ratio mass spectrometer; ICPMS, inductively coupled plasma mass spectrometry; WT, wild-type.

10.1021/bi9928952 CCC: $19.00
Published on Web 03/29/2000

plates, while the other half was plated onto LB plates supplemented with 0.4 mM IPTG. The colonies were determined to be λDE3 lysogens if the plate without IPTG contained only plaques, while the plate with IPTG contained only a "halo" of the *E. coli* lawn. Of the three colonies tested, two were determined to be true λDE3 lysogens. These cells were designated B(DE3)araD$^-$ and stored at −78 °C in 20% glycerol.

The cells were made competent by following the standard calcium chloride procedure (*3*) and transformed with the pLysS plasmid (Novagen).

Preparation of Mutant Plasmids and Enzymes. A total of 11 single-residue mutations of the 4-epimerase was made. Each of the nine tyrosine residues of the 4-epimerase was mutated to phenylalanine (Y48F, Y84F, Y121F, Y123F, Y141F, Y195F, Y219F, Y228F, and Y229F). Two histidine residues were changed to asparagine (H95N and H97N). The creation of the mutant plasmids was carried out according to the instructions of the QuikChange Site-Directed Mutagenesis Kit from Stratagene. Mutagenesis via this kit involves two complementary oligonucleotide primers with the desired nucleotide change(s) and a double-stranded plasmid template. Amplification was carried out via PCR with the use of the high-fidelity *Pfu* DNA polymerase (Stratagene).

The mutations that resulted in interesting catalytic and spectral property changes for the mutant 4-epimerases were H95N, H97N, and Y229F. The complementary oligonucleotides for the H95N mutation, as written in the 5′ to 3′ direction with the altered codon underlined, were as follows: primer 1, GGC GGC ATT GTG AAC ACA CAC TCG CGC; and primer 2, GCG CGA GTG TGT GTT CAC AAT GCC GCC. For the H97N mutation, primer 3 is C ATT GTG CAC ACA AAC TCG CGC CAC GCC and primer 4 is GGC GTG GCG CGA GTT TGT GTG CAC AAT G. For the Y229F mutation, primer 5 is GGC GCG AAG GCA TAT TTC GGG CAG TAA GGA TCC and primer 6 is GGA TCC TTA CTG CCC GAA ATA TGC CTT CGC GCC. The double-stranded DNA template used for the PCR was pLLD1 (5.3 kilobase pairs), which consisted of the wild-type araD gene in a pET3a vector (*2*). The reaction buffer, the dNTP mixture, and the *Pfu* DNA polymerase were provided by the mutagenesis kit. The PCR was carried out on a Perkin-Elmer Gene Amp PCR System 2400 under the following conditions: one cycle of 30 s at 95 °C, followed by 16 cycles of 30 s at 95 °C, 1 min at 55 °C, and 10 min and 36 s at 68 °C. One microliter of the stock solution of *Dpn* restriction enzyme was then added to the reaction mixture and the mixture incubated at 37 °C for 1 h to digest the parental (nonmutated) double-stranded DNA. The PCR product was then used to transform the *Epicurean Coli* XL-1 Blue Supercompetent Cells (Stratagene). The cells were stored at −78 °C in 20% glycerol. The Y229F mutant plasmid was designated pMVD9, the H95N plasmid pMVD10, and the H97N plasmid pMVD11.

All 11 mutant plasmids were sequenced to verify that the desired base changes had taken place and that no unintentional base changes were introduced during the PCR. The sequencing reaction was carried out according to the instructions of the ABI Prism Dye Terminator Reaction Kit, which involved two PCRs. Each reaction made use of either the T7 promoter primer or the T7 terminator primer (both from Novagen) which anneal to the promoter or to the terminator region, both of which flank the araD gene. The reaction mixtures were then sent to the University of Wisconsin Biotechnology Center for automated sequencing on the Perkin-Elmer Applied BioSystems Automated DNA Sequencer (model 377). Once the 11 mutant plasmids were sequenced, they were transformed into B(DE3)araD$^-$ cells for overexpression of the enzymes.

Screening for Slow Mutants. For comparison purposes, the wild-type 4-epimerase (*2*) was expressed and partially purified together with the 11 mutant enzymes. Overexpression by induction with IPTG was carried out in the same manner as described for the wild-type 4-epimerase (*2*). In a total of 12 vessels, each with 500 mL of LB medium containing 50 μg/mL ampicillin and 10 μg/mL chloramphenicol, the cells expressing the mutant enzymes and the wild-type 4-epimerase were grown at 37 °C for 4 h after induction with IPTG. The cells were collected by centrifugation and lysed with lysozyme. RNAse A and DNAse I were added to digest the polynucleotides. The cellular debris was separated from the crude enzyme extract by centrifugation, and the expression of the wild-type and mutant enzymes was verified by SDS−PAGE. Each mutant 4-epimerase and the wild-type enzyme were then partially purified by ammonium sulfate precipitation at 40% saturation and dialyzed twice with 250 mL of 10 mM NaHEPES (pH 7.6).

The catalytic activity of the mutant 4-epimerases and of the wild-type enzyme was tested by running all 12 activity assays in parallel. In a total reaction volume of 400 μL containing 37 mM L-Ru5P and 10 mM NaHEPES (pH 7.6), 50 μL of mutant or wild-type enzyme was added to initiate the epimerization reaction. The reaction was allowed to occur for 15 min and then stopped by removal of the enzymes by passing the reaction mixture through the Millipore Ultrafree-MC filters (MW cutoff of 10 kDa). The extent of L-Ru5P to D-Xu5P conversion was measured by the coupled enzyme assay used to acquire the pH profile of the wild-type 4-epimerase (*2*).

Overexpression and Purification of H95N, H97N, and Y229F Mutants. The large-scale overexpression and column purification of the mutant enzymes were carried out as described for the wild-type enzyme (*2*).

Preparation of Apoenzymes and Zn(II)-Substituted 4-Epimerases. Although the column-purified enzymes contained predominantly zinc in the active site, as determined by ICPMS, the enzymes were made metal-free and then reconstituted with 99.999% pure $ZnCl_2$. The apoenzymes of the H95N and H97N mutants were generated simply by once passing the column-purified enzymes through a 4 cm Chelex 100 column (2 mL volume) equilibrated in 10 mM KHEPES (pH 7.0). The purified Y229F mutant had to be dialyzed against 20 mM EDTA and 1 mM DTT (pH 7.0) for 3−4 h at room temperature to completely remove the original metals from the active site. A more detailed procedure is in the previous paper (*2*). The mutant enzymes were then reconstituted with 2 equiv of $ZnCl_2$ per active site. All metal content analyses were carried out by ICPMS at the University of Wisconsin Soil and Plant Analysis Laboratory.

Circular Dichroism and Secondary Structures of Zn(II)-Substituted Wild-Type and Mutant Enzymes. The CD spectra of the wild-type, H95N, H97N, and Y229F mutant 4-epimerase were recorded in the far-UV region (190−260 nm)

under the following conditions: 0.1 mg/mL enzyme, 10 mM potassium phosphate buffer, pH 7.5, 0.1 mM $ZnCl_2$, and 25 °C. The spectra were acquired on an Aviv CD model 62A DS spectrometer and were converted to molar ellipticity by normalizing the spectra to 0.1 mg/mL enzyme and assuming each amino acid has an average molecular mass of 110 Da/residue.

Circular Dichroism and Tertiary Structures of Zn(II)-Substituted Wild-Type and Mutant Enzymes. CD spectra were acquired in the near-UV region (240−310 nm) on an Aviv CD model 62A DS spectrometer. Three spectra were recorded for each enzyme: the apoenzyme, the Zn(II)-substituted enzyme, and the Zn(II)-substituted enzyme in the presence of L-Ru5P and D-Xu5P. Both sugars were added at equilibrium concentrations since they both have prominent CD spectra in the near-UV region (*2*). To acquire the spectrum of the tertiary structure of the Zn(II)-labeled enzyme as perturbed by substrate binding, the spectrum of the Zn(II)-labeled enzyme was recorded in the presence of L-Ru5P and D-Xu5P at equilibrium concentrations, and this spectrum was subtracted from the spectrum containing of L-Ru5P and D-Xu5P at the same concentrations. All spectra were recorded in the presence of 10 mM KHEPES (pH 7.5) since the CD spectra of L-Ru5P and D-Xu5P are pH-dependent (*2*). The sample conditions for acquiring the near-UV CD spectra were 0.6 mg/mL apoenzyme, 10 mM KHEPES (pH 7.5), 0.1 mM $ZnCl_2$, and 5 mM L-Ru5P or D-Xu5P (equilibrium concentrations). All spectra were recorded for the samples maintained at 25 °C. The spectra were converted to molar ellipticity by normalizing the spectra to 0.6 mg/mL enzyme and assuming each amino acid to have an average molecular mass of 110 Da/residue.

Steady-State Kinetics and K_m Values for Divalent Metal Ions. Steady-state kinetics was used to determined the apparent dissociation constant (K_m) of various divalent metal ions for the wild-type, H95N, H97N, and Y229F mutant 4-epimerases. The metal ions that were tested were Zn(II), Co(II), Mn(II), and Mg(II) with chloride as the counterion. All metal chlorides were from Aldrich (99.99% pure). The assay conditions were 50 mM KHEPES (pH 7.5), 5 mM L-Ru5P, metal-free 4-epimerase, and varying concentrations of each divalent metal ion. Both buffer and substrate were made metal-free by passing the solutions through a Chelex 100 column. The reaction was monitored on a Jasco J-41C CD spectrometer by measuring the change in ellipticity of L-Ru5P (*2*) at 279 nm and 22 °C. This assay detected no basal activity for the apoenzymes without the addition of divalent metal ions. Initial velocity data were fitted to the Michaelis−Menten equation using PSI Plot version 5.0 (Poly Software International).

The normalized ellipticity value of 29.3°/mM for L-Ru5P at 279 nm and pH 7.5 was used to calculate the turnover number (k_{cat}) per subunit. Enzyme concentrations were determined with the Bio-Rad protein assay using bovine serum albumin to construct a standard curve (*2*). The concentrations of the wild-type 4-epimerase (5.25×10^{-12} M) and the H95N (2.15×10^{-10} M) and H97N mutants (1.06×10^{-10} M) in the assay were at levels far below the measured K_m values for the various metals. The K_m values for the metal ions were not determined for the Y229F mutant because this mutant had very low activity and high concentrations of the enzyme were needed to observe catalytic turnover. The concentration of the Y229F mutant in the assay was higher than the K_m values for the metal ions, which made it difficult to determine the kinetic constants. Therefore, the k_{cat} values of the Y229F mutant were acquired under V_{max} conditions.

K_m Values for L-Ru5P from Various Metal-Substituted Enzymes. The K_m values for L-Ru5P were measured for the Zn(II)-, Co(II)-, Mn(II)-, and Mg(II)-substituted wild-type 4-epimerase. The reagents and enzymes required by the coupled enzyme assay (*2*) and 50 mM KHEPES (pH 7.5) were mixed together and passed through a 1 mL column of Chelating Sepharose (Pharmacia Biotech) to remove any contaminating metals. To this mixture was added 1 mM $MgCl_2$ since the coupling enzyme transketolase required the metal for activity. For each metal except Mg(II), the metal chloride (0.1 mM) was also added to the assay. However, the assay to determine the K_m of L-Ru5P with the Mg(II)-substituted wild-type enzyme contained 15 mM $MgCl_2$. L-Ru5P was varied from 0.01 to 5 mM to encompass the shift in K_m values for L-Ru5P as the divalent metal ion was changed in the wild-type enzyme. The assay was started by the addition of the wild-type enzyme that was previously reconstituted with its respective metal ion. The reaction was monitored at 22 °C. Data fitting was carried out as described above.

The same experiment was repeated for the Y229F, H97N, and H95N mutants but only as Zn(II)-substituted enzymes.

The CD assay described above could not be used for this experiment because at low L-Ru5P concentrations, the CD signal at 279 nm was too weak to allow for accurate determination of the changes in substrate concentration.

Absorption and CD Spectra of Co(II)-Substituted Wild-Type and Mutant Enzymes. The absorption and CD spectra were acquired in the visible region (400−700 nm) of the wild-type, H95N, H97N, and Y229F 4-epimerases as apoenzymes, as Co(II)-substituted enzymes, and as Co(II)-substituted enzymes in the presence of L-Ru5P. The absorption and CD spectra of the apoenzyme were acquired first in 10 mM KHEPES (pH 7.5). The spectra were recorded again after the addition of the metal ion. L-Ru5P was then added to the samples. The epimerization reaction was allowed to reach equilibrium (5 min), and the spectra were recorded again. In actuality, the high concentrations of the enzymes would cause equilibrium to be approached almost instantaneously. The additions of metal ion and L-Ru5P to the apoenzyme sample each represented a volume change of only about 1%. The absorption spectra were acquired on a Shimadzu UV−visible model UV-1601PC spectrophotometer. The sample conditions for the wild-type enzyme and the three mutants were 0.7310 mM enzyme active sites, 1.462 mM $CoCl_2$, and 3.655 mM L-Ru5P, the ratio of the components being 1:2:5. For all four enzymes, the absorption spectra in the visible region were plotted in extinction coefficient units after subtraction of the cobalt enzyme spectra, with and without substrate, from the apoenzyme "blank", which had some absorption in the region as a result of the broad 280 nm signal. The CD spectra were acquired on the Aviv CD model 62A DS spectrometer. The sample conditions for all four enzymes were 1 mM active sites, 2 mM $CoCl_2$, and 5 mM L-Ru5P. The CD spectra were normalized to the concentration of active sites in the samples.

All samples were maintained at 25 °C during acquisition of the spectra.

Aldolase Activity of Zn(II)-Substituted Wild-Type and Mutant Enzymes. Activity of the 4-epimerase-catalyzed aldol condensation reaction between dihydroxyacetone and glycolaldehyde phosphate was determined as described by Johnson and Tanner (*4*). Dihydroxyacetone was purchased from Sigma. Glycolaldehyde phosphate was synthesized in the following manner. In a total volume of 150 mL, 10 mmol of D,L-glycerol phosphate (Sigma) and 11 mmol of sodium periodate were mixed. The pH of the solution was adjusted to 6.0 with 1 M HCl, and the reaction was allowed to go to completion, which required 12 h at 37 °C, as determined by ^{1}H NMR. The reaction was quenched with 2 mmol of glycerol, which consumed the unreacted periodate. The pH was readjusted to 7.0 with 1 M NaOH, and 22 mmol of $BaCl_2$ was added to the solution. Immediately, a white precipitate of barium iodate was observed. The reaction mixture was chilled on ice for 1 h to ensure that all the barium iodate had precipitated. The precipitate was collected by centrifugation and discarded. Four volumes of absolute ethanol was added to the solution to precipitate the barium salt of glycolaldehyde phosphate. The barium glycolaldehyde phosphate was collected by centrifugation and dried under vacuum to remove water and ethanol. The barium glycolaldehyde phosphate was redissolved in water, and the barium ions were exchanged for protons by passing the solution through a column of Dowex AG50X8 (H^+ form). The pH of the solution was readjusted to 7.0 with 1 M NaOH. The sodium glycolaldehyde phosphate solution was concentrated and stored frozen at −20 °C. Although this synthesis of glycolaldehyde phosphate is different from the literature method (*5*), the ^{1}H NMR spectrum of the compound showed very similar chemical shifts and coupling constants.

The aldol condensation reaction between dihydroxyacetone and glycolaldehyde phosphate was carried out under the following conditions (*4*): 0.5 mg of apoenzyme (wild type, H95N, H97N, or Y229F), 50 mM KHEPES (pH 7.5), 0.1 mM $ZnCl_2$, 5 mM glycolaldehyde phosphate, and 50 mM dihydroxyacetone, in a total volume of 1 mL. At time intervals of about 2 h, aliquots of 50 μL were taken from each reaction mixture and assayed for L-Ru5P and D-Xu5P using the coupled enzyme assay (*2*).

EPR Spectra of Mn(II)-Substituted Wild-Type 4-Epimerase. The Q-band EPR spectra for the Mn(II)-substituted wild-type 4-epimerase with and without the substrates were recorded. The spectra for a 10 μL sample which consisted of 5 mM 4-epimerase active sites and 2.65 mM of $MnCl_2$ (99.999% pure) were recorded. In three separate samples, L-Ru5P was added to titrate the active site such that the final concentrations of the enzyme and substrate were in ratios of 1:1, 1:4, and 1:17 and a spectrum of each was taken.

Water Ligand Count by EPR. The number of water ligands on Mn^{2+} in the enzyme−Mn^{2+} complex was determined by spectral subtraction (*6*−*9*) of the spectrum obtained in $H_2{}^{17}O$. The EPR signals of Mn^{2+} complexes containing ^{17}O ligands are inhomogeneously broadened by coupling between the Mn^{2+} electron spin and the nuclear spin ($I = {}^5/_2$) of ^{17}O (*6*). When water containing less than 100% ^{17}O is used, the sample contains a mixture of species bearing different numbers of $H_2{}^{17}O$ ligands. Species with no $H_2{}^{17}O$ ligands contribute an EPR signal identical to the signal obtained in normal water. The fractional contribution (F_n) of this unperturbed signal to the observed EPR signal of a sample in $H_2{}^{17}O$ depends on the enrichment (E) of ^{17}O and the number (n) of H_2O ligands in the complex according to eq 1.

$$F_n = (1 - E)^n \quad (1)$$

To determine the number of water ligands in a complex, concentration-matched samples are prepared in $H_2{}^{17}O$ or $H_2{}^{16}O$, and their EPR spectra are recorded. Different fractions (F_n, eq 1) of the $H_2{}^{16}O$ spectrum, corresponding to different numbers of water ligands, are subtracted from the $H_2{}^{17}O$ spectrum. The number of water ligands is the smallest n (largest F_n) to give a subtraction that just cancels the $H_2{}^{16}O$ portion of the spectrum without creating a negative image of the $H_2{}^{16}O$ spectrum in the difference.

EPR samples for the water count were prepared by mixing 8 μL of Mn(II)-substituted wild-type 4-epimerase (5 mM active sites and 2.65 mM $MnCl_2$) and 4 μL of H_2O or $H_2{}^{17}O$ (52.8 at. % ^{17}O, Isotec Inc.). All Q-band (35 GHz) EPR spectra were acquired with a Varian E109Q spectrometer. The sample temperature was maintained at 4 ± 1 °C with a Varian flow dewar and temperature controller. The spectrometer was interfaced with an AT microcomputer for data acquisition. Spectra were resolution enhanced by Fourier deconvolution methods (*10*, *11*) to increase the contrast between the difference spectra.

RESULTS

Screening for Slow Mutants. Nine tyrosine to phenylalanine mutant 4-epimerases (Y48F, Y84F, Y121F, Y123F, Y141F, Y195F, Y219F, Y228F, and Y229F) and the two histidine to asparagine mutants (H95N and H97N) were tested in the coupled assay (see Experimental Procedures). During the 15 min incubation, all reactions reached equilibrium except Y48F (85%), Y228F (64%), Y229F (3.3%), H95N (23%), and H97N (68%) (percentages are of approach to equilibrium). Both the Y229F and H95N mutants had catalytic activities significantly lower than that of the WT 4-epimerase, while the other tyrosine mutants had activity not greatly different from that of the WT enzyme. The H97N mutant was slightly slower than the WT enzyme.

Circular Dichroism and Secondary Structures of Wild-Type and Mutant Enzymes. The far-UV (190−260 nm) CD spectra of the WT epimerase and the H95N, H97N, and Y229F mutants were nearly identical, indicating that the mutant 4-epimerases have secondary structures that are essentially the same as the WT enzyme.

Circular Dichroism and Tertiary Structures of Zn(II)-Substituted Wild-Type and Mutant Enzymes. The near-UV (240−310 nm) CD spectra of the WT 4-epimerase (Figure 1A) and the Y229F (Figure 1B), H97N (Figure 2A), and H95N (Figure 2B) mutants can be categorized into two groups, with the WT epimerase and the Y229F mutant in one group and the histidine mutants in the other. It is apparent from Figures 1 and 2 that the CD spectra of the apoenzyme and of the enzyme with Zn(II) present are very similar. However, upon addition of the substrate/product mixture to the Zn(II)-substituted enzymes, there were noticeable changes in the spectra, with the band at 266 nm increasing in

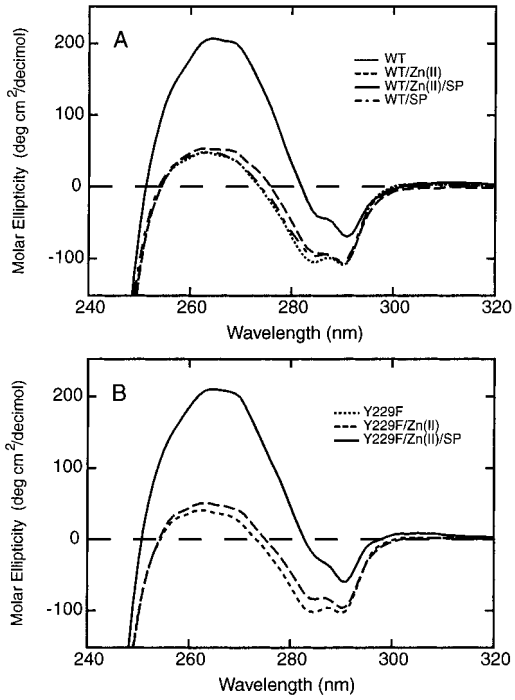

FIGURE 1: Near-UV spectra of (A) wild-type and (B) Y229F 4-epimerases as apoenzymes, as Zn(II)-substituted enzymes, and as zinc enzymes in the presence of substrate and product. See Experimental Procedures for conditions of data collection.

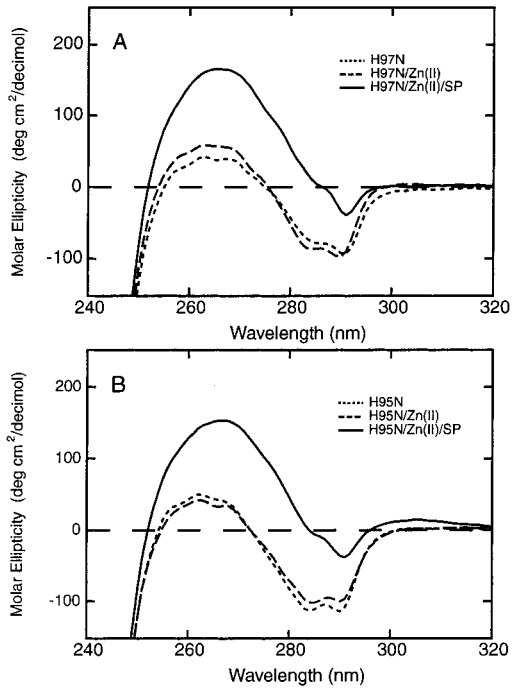

FIGURE 2: Near-UV spectra of (A) H97N and (B) H95N 4-epimerases as apoenzymes, as Zn(II)-substituted enzymes, and as zinc enzymes in the presence of substrate and product. See Experimental Procedures for conditions of data collection.

ellipticity and the band at 290 nm and the shoulder at 286 nm decreasing in ellipticity. The addition of the substrate/product mixture appeared to increase the ellipticity of the band at 266 nm for the WT enzyme and the Y229F mutant to a greater degree than with the H97N and H95N mutants, while the band at 290 nm resulted in a greater decrease in ellipiticity for the H97N and H95N mutants than for the WT enzyme or the Y229F mutant. If the reactants were added to the apoenzyme without Zn(II) being present, the spectrum did not change (Figure 1A).

Steady-State Kinetics and K_m Values of Divalent Metal Ions. The apparent dissociation constants (K_m) of the various divalent metal ions [Zn(II), Co(II), Mn(II), and Mg(II)] for the WT epimerase and mutant enzymes are listed in Table 1, along with k_{cat} and k_{cat}/K_m values. Table 1 shows that WT enzyme had the greatest activity, while the H97N, H95N, and Y229F mutants had 10, 1, and 0.1% of the WT activity, respectively. Although there does not appear to be a trend in k_{cat} values for the various metals among the different enzymes, there is a trend in K_m and k_{cat}/K_m values. For each enzyme except the Y229F mutant, the K_m values increased from Zn(II) to Mg(II) and increased for each metal from the WT enzyme to the H95N mutant. The K_m value for Mg(II) for the H97N mutant was difficult to measure because it was very large, possibly in the molar range. However, the H97N mutant did display some activity in the presence of Mg(II). The H95N mutant displayed no activity in the presence of Mg(II). For each enzyme, the k_{cat}/K_m values were the highest for Zn(II) and decreased to the lowest value for Mg(II). For each metal, the k_{cat}/K_m values were highest for the WT enzyme and lowest for the H95N mutant.

K_m Values for L-Ru5P with Metal-Substituted Enzymes. As indicated by Table 2, the K_m value for L-Ru5P is smallest for the Zn(II)-substituted WT enzyme and the values increase from Zn(II) to Mg(II). The k_{cat}/K_m value is the largest for the Zn(II)-substituted WT enzyme, and the values decrease from Zn(II) to Mg(II). There does not appear to be a trend in the k_{cat} values.

Table 3 shows that the Zn(II)-substituted mutant enzymes exhibit larger K_m values and smaller k_{cat} and k_{cat}/K_m values than the WT enzyme.

Absorption and CD Spectra of Co(II)-Substituted WT and Mutant Enzymes. The absorption and CD spectra of the Co(II)-substituted enzymes in the visible region (400−700 nm) show that the spectra of the WT epimerase (Figure 3) and the Y229F mutant (Figure 4) are very similar, while the spectra of the H97N (Figure 5) and H95N (Figure 6) mutants are unique to each enzyme. The absorption spectra of the cobalt enzymes without substrate show that each enzyme has a shoulder at 476 nm and a maximum at 508 nm. The extinction coefficients for the maxima are all approximately 50 M^{-1} cm^{-1}. The CD spectra of the cobalt enzymes without substrate are unique to each enzyme, except between the WT enzyme and the Y229F mutant, and the bands do not appear to have a precise correspondence in wavelength to the absorption spectra.

The addition of substrate to the cobalt enzymes caused a red shift and an increase in intensity of the bands in the absorption spectra. A similar change is also observed in the CD spectra. The changes are nearly identical for the WT enzyme and the Y229F mutant but are different in shape and magnitude for the H97N and H95N mutants. The addition of the substrate to the cobalt WT and cobalt Y229F enzymes resulted in the appearance of a shoulder a 497 nm and a maximum at 556 nm, with the extinction coefficients of the maximum of 160 and 174 M^{-1} cm^{-1}, respectively. The CD spectra of these two enzymes are essentially mirror images of the absorption spectra, with a precise correspondence in the wavelength of the bands. The molar

Table 1: Kinetic Constants for Different Metal Ions for WT and Mutant L-Ru5P 4-Epimerases[a]

	$ZnCl_2$	$CoCl_2$	$MnCl_2$	$MgCl_2$
wild-type				
K_m (μM)	0.17 ± 0.02	0.29 ± 0.05	0.54 ± 0.11	1350 ± 420
k_{cat} (s^{-1})	16.7 ± 0.4	24.3 ± 0.9	37.2 ± 1.9	0.855 ± 0.056
k_{cat}/K_m (μM^{-1} s^{-1})	98.2 ± 10.6	83.8 ± 14.6	68.9 ± 13.5	0.000633 ± 0.000191
Y229F				
K_m (μM)	–	–	–	–
k_{cat} (s^{-1})	0.0111	0.307	0.0557	0.0041
k_{cat}/K_m (μM^{-1} s^{-1})	–	–	–	–
H97N				
K_m (μM)	0.53 ± 0.04	1.67 ± 0.21	100 ± 14	–
k_{cat} (s^{-1})	1.77 ± 0.05	2.14 ± 0.07	0.737 ± 0.037	0.0787
k_{cat}/K_m (μM^{-1} s^{-1})	3.34 ± 0.25	1.28 ± 0.16	0.00737 ± 0.00103	–
H95N				
K_m (μM)	2.02 ± 0.43	60 ± 5	3170 ± 530	–
k_{cat} (s^{-1})	0.190 ± 0.009	0.562 ± 0.032	0.380 ± 0.018	0
k_{cat}/K_m (μM^{-1} s^{-1})	0.094 ± 0.020	0.00937 ± 0.00078	0.00012 ± 0.00002	–

[a] Reaction mixtures contained 5 mM L-Ru5P, 50 mM KHEPES (pH 7.5), and metal-free enzyme.

Table 2: Kinetic Constants for L-Ru5P with WT Epimerase and Different Metal Ions[a]

	$ZnCl_2$	$CoCl_2$	$MnCl_2$	$MgCl_2$
K_m (mM)	0.0471 ± 0.0066	0.110 ± 0.011	0.415 ± 0.072	0.493 ± 0.123
k_{cat} (s^{-1})	17.3 ± 0.5	21.8 ± 0.5	36.5 ± 1.5	0.502 ± 0.041
k_{cat}/K_m (mM^{-1} s^{-1})	367 ± 51	198 ± 20	87.9 ± 15.2	1.02 ± 0.25

[a] Reaction mixtures contained 0.1 mM metal ion (as Cl^-), except 15 mM $MgCl_2$, 50 mM KHEPES (pH 7.5), and metal-free enzyme.

Table 3: Kinetic Constants for L-Ru5P with Y229F, H97N, and H95N Mutants[a]

	Zn(II)-Y229F	Zn(II)-H97N	Zn(II)-H95N
K_m (mM)	0.129 ± 0.012	0.132 ± 0.021	0.091 ± 0.014
k_{cat} (s^{-1})	0.0118 ± 0.0003	2.01 ± 0.09	0.183 ± 0.007
k_{cat}/K_m (mM^{-1} s^{-1})	0.0915 ± 0.0085	15.2 ± 2.4	2.01 ± 0.31

[a] Reaction mixtures contained 0.1 mM $ZnCl_2$, 50 mM KHEPES (pH 7.5), and metal-free enzymes.

ellipticity of the band at 556 nm for the WT enzyme is -1842 deg cm^2 $dmol^{-1}$.

The absorption and CD spectra of the cobalt H97N and H95N mutants with substrate present are unique to each enzyme. The intensity of the bands in both the absorption and CD spectra is not as great as for the WT enzyme or the Y229F mutant. However, like the bands of these two other enzymes, the bands correspond well in wavelength between the absorption and CD spectra.

As a control experiment, absorption and CD spectra for the $CoCl_2$ and substrate mixture without enzyme present were recorded. The experiment showed no increase in absorption intensity above the very weak band of the aqua−cobalt complex at 510 nm and no generation of bands in the CD spectrum (not shown).

Aldolase Activity of Zn(II)-Substituted WT and Mutant Enzymes. The 4-epimerase catalyzed the aldol condensation reaction between dihydroxyacetone and glycolaldehyde phosphate (Figure 7) was catalyzed at nearly identical initial velocities by all four enzymes that were tested. As the reaction proceeded, however, the reaction rate fell off due to competition from the much more tightly bound L-Ru5P and D-Xu5P that formed. This effect was greater for the WT enzyme which has the lowest K_m (0.5 mM), intermediate for the H95N mutant (K_m = 0.9 mM), and least for the H97N and Y229F mutants (K_m = 0.13 mM). The initial rate at pH 7.5 of 1.6×10^{-3} s^{-1} was 0.003% of the WT epimerase rate, and 0.03, 0.2, and 4% of the epimerase rates of the H97N, H95N, and Y229F mutants, respectively. The rate at pH 8.0 was 1.7 times the rate at pH 7.0, which suggests that the dienolate of dihydroxyacetone is not the sole substrate. Presumably, either the keto or enol forms of dihydroxyacetone are the major forms that bind and react.

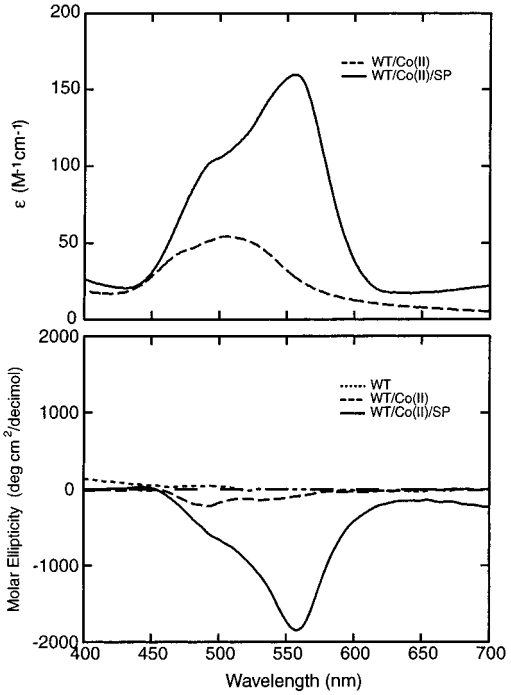

FIGURE 3: Absorption and CD spectra of wild-type L-Ru5P 4-epimerase in the visible region as an apoenzyme, as a Co(II)-substituted enzyme, and as a cobalt enzyme in the presence of substrate and product. See Experimental Procedures for conditions of data collection.

EPR Spectra of Mn(II)-Substituted WT 4-Epimerase. The EPR spectrum of the Mn(II)-substituted WT epimerase

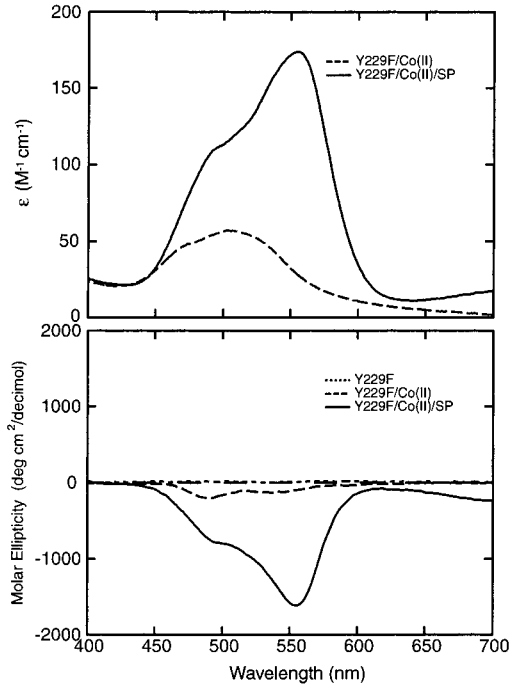

FIGURE 4: Absorption and CD spectra of Y229F 4-epimerase in the visible region as an apoenzyme, as a Co(II)-substituted enzyme, and as a cobalt enzyme in the presence of substrate and product. See Experimental Procedures for conditions of data collection.

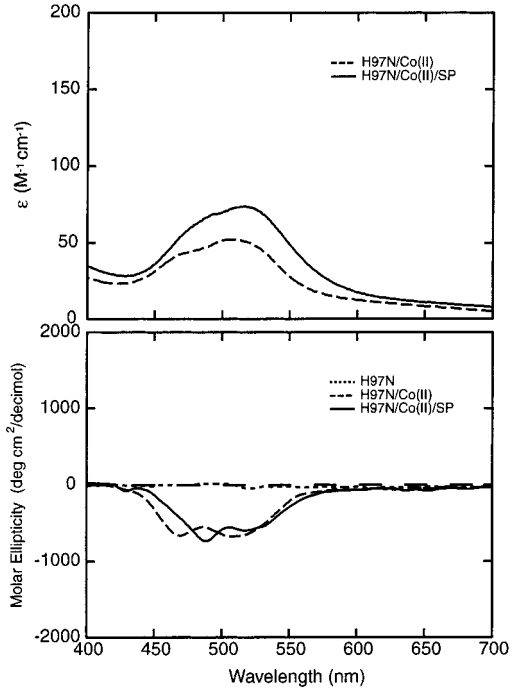

FIGURE 5: Absorption and CD spectra of H97N 4-epimerase in the visible region as an apoenzyme, as a Co(II)-substituted enzyme, and as a cobalt enzyme in the presence of substrate and product. See Experimental Procedures for conditions of data collection.

(Figure 8A) exhibits a sextet with the ^{55}Mn hyperfine coupling constant of about 90 G. The addition of the L-Ru5P to the manganese enzyme at a ratio of 1:1 resulted in a spectrum with a broad feature partially hidden by the sextet with the sextet reduced to one-tenth of its original intensity (Figure 8B). Subsequent titration of the active site with higher levels of substrate, 1:4 and 1:17, resulted in spectra that were essentially the same as Figure 8B (not shown).

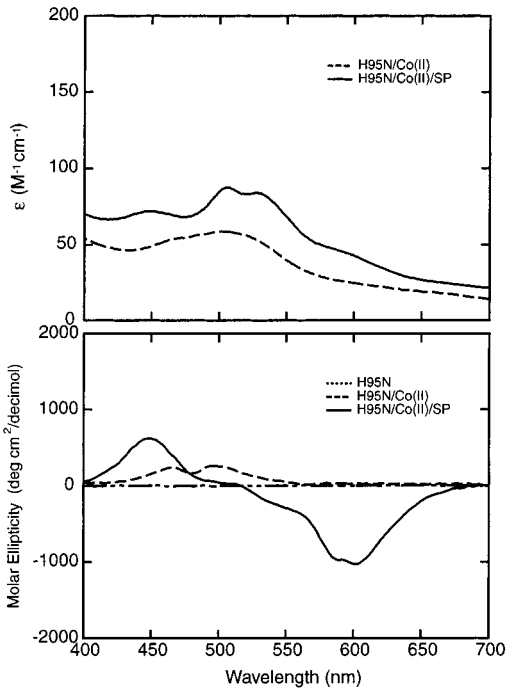

FIGURE 6: Absorption and CD spectra of H95N 4-epimerase in the visible region as an apoenzyme, as a Co(II)-substituted enzyme, and as a cobalt enzyme in the presence of substrate and product. See Experimental Procedures for conditions of data collection.

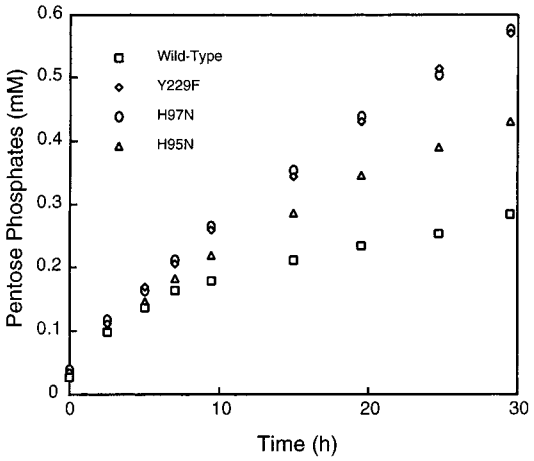

FIGURE 7: Aldolase activity of wild-type and mutant L-Ru5P 4-epimerases, with 50 mM dihydroxyacetone and 5 mM glycolaldehyde phosphate. The generation of L-Ru5P and D-Xu5P was detected by the coupled enzyme assay (see Experimental Procedures for details). Reaction mixtures contained enzyme (each at 0.5 mg/mL) and 50 mM KHEPES (pH 7.5). The inital rates were 1.6×10^{-3} s^{-1}.

Water Ligand Count by EPR. The hydration number of Mn(II) in the complex with the WT epimerase was determined by quantitative analysis of the ^{17}O-induced inhomogeneous broadening of the EPR spectrum of the manganese enzyme in ^{17}O-enriched water. Figure 9 represents the difference spectra between the EPR spectrum of the Mn(II)-substituted WT enzyme obtained in enriched water and the spectrum of the enzyme obtained in normal water. The spectrum of Figure 9A was created with the assumption that one water molecule is bound to the Mn(II), while Figure 10B assumes two water molecules and Figure 10C three water molecules. The arrows indicate the location of the negative image of the spectrum of the sample in unenriched

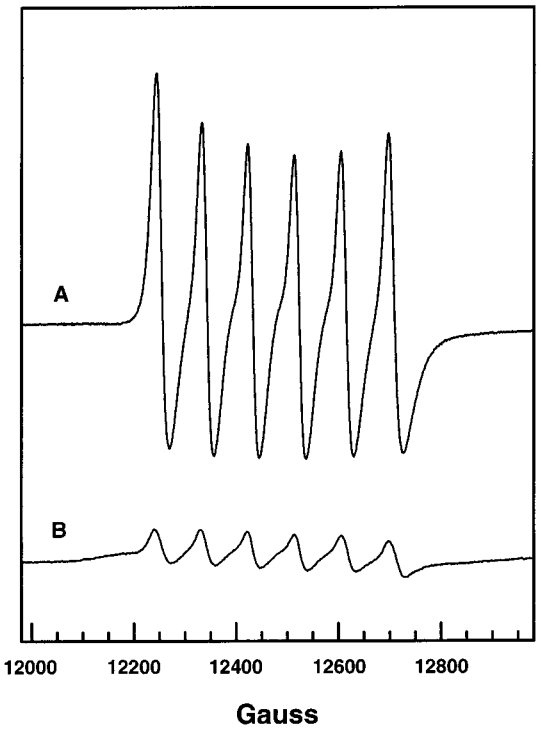

FIGURE 8: EPR spectra of Mn(II)-substituted wild-type 4-epimerase in the (A) absence and (B) presence of substrate and product. See Experimental Procedures for conditions of data collection.

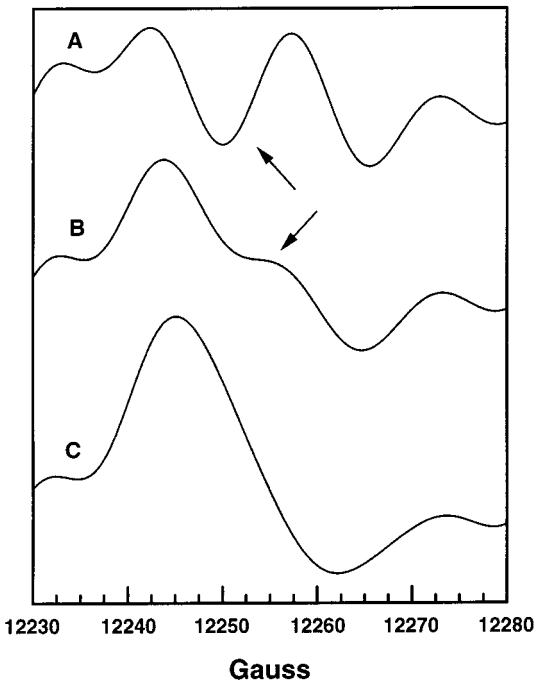

FIGURE 9: Water ligand count of Mn(II)-substituted wild-type 4-epimerase by EPR. See Experimental Procedures for conditions of data collection.

water in the difference spectrum corresponding to one or two water ligands. This negative image is absent in the difference spectrum corresponding to three water ligands, indicating that the correct assumption is three water ligands.

DISCUSSION

Information from the X-ray crystal structure of L-Fuc1P aldolase (*12*−*14*) and the finding of sequence alignments among L-Ru5P 4-epimerase, L-Fuc1P aldolase, and L-Rhu1P aldolase (*2*) suggested that Asp76, His95, His97, and His171 of the 4-epimerase are involved in the binding of the divalent metal ion. Also, the crystal structure of L-Fuc1P aldolase in the presence of the inhibitor phosphoglycolohydroxamate suggests that Tyr113 of the aldolase may be involved as the general acid and base residue in the enzyme-catalyzed aldol cleavage and condensation reactions (*14*). These observations led to the site-specific mutagenesis work described in this paper, namely, conservative residue changes, histidine to asparagine, of some of the potential metal ion ligand residues of the 4-epimerase, and tyrosine to phenylalanine for each tyrosine, to search for tyrosines that may be involved in catalysis. The structure of the epimerase has recently been determined to 2.4 Å resolution by X-ray crystallography; H95, H97, and H171 *are* metal ion ligands, while Asp76 is not (N. Strynadka, pesonal communication).

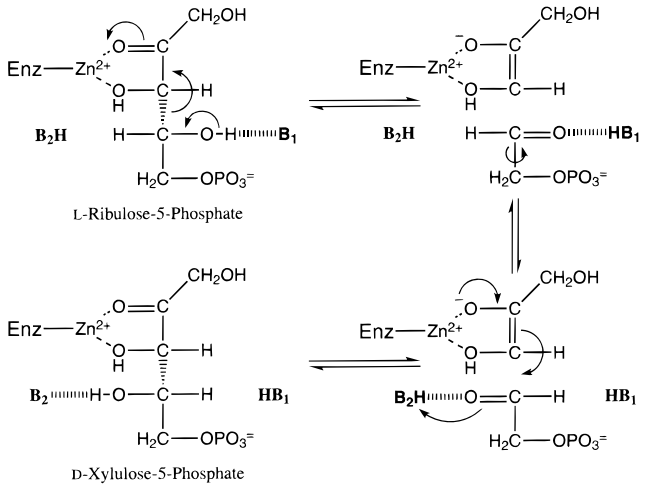

FIGURE 10: Proposed mechanism of the L-Ru5P 4-epimerase-catalyzed reaction. The diagram depicts an aldol cleavage−condensation mechanism for conversion of L-Ru5P to D-Xu5P that involves substrate to metal binding and a cis enediolate-stabilized intermediate.

A total of 11 mutants of the 4-epimerase were created, and three (Y229F, H97N, and H95N) were found to exhibit slow catalytic activity as determined by the screening process. Mutation of the other tyrosines in the enzyme had little effect. The mutations at Asp76 and His171 were not studied in this set of experiments.

The far-UV CD spectra of the mutant 4-epimerases and of the WT enzyme show that the mutant enzymes have secondary structures essentially identical to those of the wild-type enzyme. Although the far-UV spectrum will provide information about the secondary structure of enzyme, the near-UV CD spectrum, which reflects the tertiary structure of the enzyme, is believed to be a more sensitive method for detecting structural changes. The bands in a near-UV CD spectrum arise from tryptophanyl, tyrosyl, phenylalanyl, cystinyl, and certain prosthetic groups. If a chromophore does not have a plane of symmetry or a center of inversion, it is inherently optically active. For chromophores having a plane of symmetry or a center of inversion, CD absorption occurs only if these chromophores are perturbed by their surroundings. Thus, the aromatic rings of tyrosyl, tryptophanyl, and phenylalanyl groups gain near-UV CD bands through interactions with nearby residues in the protein (*15*).

The chromophores that are of concern in the L-Ru5P 4-epimerase are its nine tyrosines, four tryptophans, and six

phenylalanines. Although it would be difficult to assign each CD band in the near-UV region, one can still gain some qualitative information about structure by visual inspection of the spectra. It is apparent from the spectra that the WT enzyme (Figure 1A) and the Y229F mutant (Figure 1B) are structurally similar to each other, while the H97N (Figure 2A) and H95N (Figure 2B) mutants are similar to one another but different from the WT enzyme and the Y229F mutant. For all four enzymes, the similarity of the spectra of the apoenzymes and the Zn(II)-substituted enzymes (without the substrate/product mixture) indicates that zinc may play only a catalytic role and not a structural role in the active site of the enzyme (*16*), since the removal of the metal ion from the enzyme does not change its tertiary structure, but without the metal the enzyme has no activity (below). Before the addition of the substrate/product mixture, there appears to be little difference in the tertiary structures of the apoenzyme and the zinc enzyme.

However, upon addition of reactants to the zinc enzymes, the H97N and H95N mutants undergo structural changes that are different from those undergone by the WT enzyme and Y229F mutant. This observation, together with others (below), suggests that the histidine residues are involved in metal binding and that the Tyr229 residue is not, and the recently determined X-ray structure confirms this (N. Strynadka, personal communication).

The lack of change in the spectrum of the apoenzyme upon addition of the reactants without Zn(II) (Figure 1A) present suggests that the Zn(II) binds to the enzyme before the substrate does.

The finding of different CD spectra for L-Ru5P and D-Xu5P (*2*) allowed for a more direct measurement of the K_m and k_{cat} values without the use of coupling enzymes. As indicated by Table 1, the higher K_m values of the divalent metal ions for both the H97N and H95N mutants as compared with those of the WT enzyme suggest that the mutation of the two histidine residues results in weaker binding of the metal ions. Though the K_m values could not be measured for the Y229F mutant, it is believed that its K_m values are close to those of the WT enzyme since removal of the metal ions from the Y229F mutant during apoenzyme preparation required dialysis with EDTA, as was needed for the WT enzyme. The histidine mutants, which bind the metal ions less tightly, were made metal-free simply by passing the enzymes through a Chelex 100 column.

It is interesting to note that the K_m values of the metal ions appear to follow the reciprocal of the Irving−Williams series [Ba(II) < Sr(II) < Ca(II) < Mg(II) < Mn(II) < Fe(II) < Co(II) < Ni(II) < Cu(II) > Zn(II)], a measure of the formation constants between chelator and metal ions for the metals listed (*17*). This observation is consistent with the concept that the apparent dissociation constant (K_m) is a thermodynamic measure of the degree of stability of the enzyme for substrate binding. In this case, the "substrate" is the metal ion. The same trend in the Irving−Williams series is also observed in the K_m values for L-Ru5P when various metals are substituted in the WT enzyme (Table 2). It would appear that the efficiency of the enzyme, as denoted by the k_{cat}/K_m value, is dependent to some degree on the strength of the substrate to metal binding.

Further evidence that His97 and His95 may be metal ligands is found in the absorption and CD spectra of the Co(II)-substituted enzymes in the visible region. It is evident when comparing the spectra from Figures 3−6 that in the presence or absence of reactants the absorption and CD spectra of the H97N (Figure 5) and H95N (Figure 6) mutants are different from the spectra of the WT enzyme (Figure 3) and the Y229F mutant (Figure 4). From the CD spectra, it would appear that the mutations at residues His97 and His95 have caused a change in the symmetry of the coordination sphere around Co(II). With the reactants present, the difference in the spectra between the histidine mutants and the other two enzymes becomes even more apparent. This suggests that the mutation of the histidine residues has also changed the coordination geometry of the Co(II)−substrate complex. The spectroscopic data for the H97N and H95N mutants also support the finding that the mutation from a stronger metal binding to a weaker metal binding residue, histidine to asparagine, results in higher K_m values for metal ions (Table 1).

The extinction coefficient of the metal complex can provide some information about the coordination geometry of the complex (*18*−*20*). Tabulation of the extinction coefficients of inorganic Co(II) complexes with known coordination numbers (*19*, *20*) shows that four-coordinate complexes have values that are generally greater than 300 M^{-1} cm^{-1}, while five-coordinate complexes have values between 50 and 225 M^{-1} cm^{-1}. Six-coordinate Co(II) complexes generally have lower absorptivity in the visible region (*20*). Since the extinction coefficients of the cobalt wild-type 4-epimerase and the three mutants (Figures 3−6) are all around 50 M^{-1} cm^{-1} with no substrate present and between 74 and 174 M^{-1} cm^{-1} with substrate present, it may be that the coordination number is five. While this judgment on the coordination number is more definitive for the Co(II)-substituted enzymes in the presence of the substrate, particularly for the WT enzyme and the Y229F mutant, the same conclusion is more difficult to make with the cobalt enzymes in the absence of the substrate. The value of 50 M^{-1} cm^{-1} may correspond to a coordination number of six.

The spectroscopic and steady-state kinetic information acquired thus far have not produced conclusive evidence for the role of Tyr229 in the epimerization reaction. However, the Y229F mutant spectroscopically behaves much like the WT enzyme and not like the histidine mutants, which suggests that residue Tyr229 is not a metal ligand. Additional experiments are needed to determine the cause of the reduction of the turnover number due to the change in this residue [it is disordered in the current X-ray structure (N. Strynadka, personal communication)]. Although the role of residue Tyr228 was not investigated in detail in this work, some catalytic rate reduction was observed for the Y228F mutant during the process of screening for slow mutants. The reduction in activity was similar to that of the H97N mutant.

Evidence from the EPR spectra of the Mn(II)-substituted WT enzyme supports the data from the absorption and CD spectra of the Co(II)-substituted enzymes. The sextet in the absence of substrate (Figure 8A) originates from an isolated Mn(II) ($S = {}^5/_2$) bound in an enzyme complex such that the dominant EPR signals arise from the $m_s = {}^1/_2 \leftrightarrow m_s = -{}^1/_2$ electron spin (fine structure) transition. This transition is split into a sextet by hyperfine coupling to the nuclear spin of ^{55}Mn ($I = {}^5/_2$) (*9*). Upon addition of the substrate to the manganese 4-epimerase (Figure 8B), a broad feature beneath the sextet was introduced and the sextet was reduced to one-

tenth the intensity. This suggests that in the presence of the substrate, the coordination sphere around the metal has been changed, perhaps due to substrate binding to manganese.

The ^{55}Mn hyperfine coupling constant, $|A|$, of about 90 G (0.0084 cm^{-1}) (Figure 8A) is indicative of a complex with octahedral geometry. Since the extinction coefficient of the cobalt−enzyme complex suggests that the coordination number is five, the active site of the 4-epimerase appears to allow a variety of coordination geometries while retaining its catalytic ability. Previous work with carboxypeptidase A showed that the enzyme retained essentially full catalytic activity when its Zn(II) metal was substituted with Co(II) or Ni(II), even though it was determined that the Zn(II)-substituted carboxypeptidase has tetrahedral geometry, the Co(II)-substituted enzyme has pentacoordinate geometry, and the Ni(II)-substituted enzyme has hexacoordinate geometry (*19*, *21*, *22*).

The water count experiment (Figure 9) shows that the Mn(II) in the metal−enzyme complex is hydrated by three water molecules. Because the EPR experiments showed that the enzyme-bound Mn(II) has octahedral geometry, with three sites occupied by water molecules, the 4-epimerase must bind its divalent metal ion with only three residues. This finding is consistent with the X-ray structure which shows that His95, His97, and His171 are metal ion ligands (N. Strynadka, personal communication).

The spectroscopic and steady-state kinetic evidence shows that the L-Ru5P 4-epimerase has a requirement for divalent metal cations, Zn(II) in particular, for catalysis and suggests that the mechanism for the enzyme-catalyzed epimerization reaction involves binding of substrate to a divalent metal ion. The current mutagenesis work supports the sequence alignment data, which suggest that His95 and His97 are metal binding residues. Together with the isotope effect data, which show that the enzyme-catalyzed epimerization occurs by the aldol cleavage and condensation reaction (*2*), the aggregate data point to the mechanism of epimerization summarized in Figure 10.

In the substrate−enzyme complex, L-Ru5P binds to the divalent metal ion in a bidentate cis configuration. The metal ion is held in place by three residues on the enzyme, two of which are His95 and His97. A basic residue abstracts the proton on the hydroxyl group on C-4 and initiates a series of bond rearrangements that results in the cleavage of the C−C bond between C-3 and C-4. Two enzyme-bound intermediates are formed, dihydroxyacetone and glycolaldehyde phosphate, with the dihydroxyacetone bound in a cis enediolate configuration to the Zn(II). The C−C bond between C-4 and C-5 rotates 180°, and another series of bond rearrangements occurs to re-form the bond between C-3 and C-4. An acidic residue donates a proton to the oxygen on C-4 to complete the reaction and produce D-Xu5P. It is unlikely that the same group acts as both a general acid and general base in the reaction. Tyr229 may be one of these.

The information collected in this work presents an opportunity to design the L-Ru5P 4-epimerase by site-specific mutagenesis into an aldolase that can generate pentose phosphates with stereospecificity at C-4. Currently, carbohydrate synthesis with class I or class II aldolases necessitates the use of dihydroxyacetone phosphate for the condensation reaction. The product of the reaction is a sugar that is phosphorylated at C-1. As has been shown previously (*4*) and in this work, the 4-epimerase has inherent aldolase activity, although the mutants in the study presented here all showed the same initial rate for this activity (Figure 7). The advantage of using a variant of the 4-epimerase to produce phosphorylated carbohydrates is that dihydroxyacetone can be used for the reaction and the product of the reaction is phosphorylated at C-5. The Y229F mutant is a likely candidate for further mutagenesis work with which to generate a stereospecific dihydroxyacetone-utilizing aldolase, since it has been shown to have low epimerase activity (Tables 1 and 2) and significant aldolase activity (Figure 7).

ACKNOWLEDGMENT

We thank Dr. Nancy Lee of the University of California at Santa Barbara for her generous gift of the pNL16 plasmid and the *E. coli* B/r D^{-139} strain and Dr. Darrell McCaslin of the University of Wisconsin−Madison Biophysics Instrumentation Facility for his helpful suggestions and comments on the CD spectroscopy portion of this paper.

REFERENCES

1. Englesberg, E., Anderson, R. L., Weinberg, R., Lee, N., Hoffee, P., Huttenhauer, G., and Boyer, H. (1962) *J. Bacteriol. 84*, 137−146.
2. Lee, L. V., Vu, M. V., and Cleland, W. W. (2000) *Biochemistry 39*, 4808−4820.
3. Maniatis, T., Fritsch, E. F., and Sambrook, J. (1982) *Molecular Cloning*, Cold Spring Harbor Laboratory Press, Cold Spring Harbor, NY.
4. Johnson, A. E., and Tanner, M. E. (1998) *Biochemistry 37*, 5746−5754.
5. Pitsch, S., Pombo-Villar, E., and Eschenmoser, A. (1994) *Helv. Chim. Acta 77*, 2251−2285.
6. Reed, G. H., and Leyh, T. S. (1980) *Biochemistry 19*, 5472−5480.
7. Lodato, D. T., and Reed, G. H. (1987) *Biochemsitry 26*, 2243−2250.
8. Smithers, G. W., Poe, M., Latwesen, D. G., and Reed, G. H. (1990) *Arch. Biochem. Biophys. 280*, 416−420.
9. Poyner, R. R., and Reed, G. H. (1992) *Biochemistry 31*, 7166−7173.
10. Kauppinen, J. K., Moffatt, D. J., Mantsch, H. H., and Cameron, D. G. (1981) *Appl. Spectrosc. 35*, 271−276.
11. Latwesen, D. G., Poe, M., Leigh, J. S., and Reed, G. H. (1992) *Biochemistry 31*, 4946−4950.
12. Dreyer, M. K., and Schulz, G. E. (1993) *J. Mol. Biol. 231*, 549−553.
13. Dreyer, M. K., and Schulz, G. E. (1996) *Acta Crystallogr. D52*, 1082−1091.
14. Dreyer, M. K., and Schulz, G. E. (1996) *J. Mol. Biol. 259*, 458−466.
15. Strickland, E. H. (1974) *CRC Crit. Rev. Biochem. 2*, 113−175.
16. Vallee, B. L., and Galdes, A. (1984) *Adv. Enzymol. 56*, 283−430.
17. Shriver, D. F., Atkins, P. W., and Langford, C. H. (1990) *Inorganic Chemistry*, W. H. Freeman and Co., New York.
18. Latt, S. A., and Vallee, B. L. (1971) *Biochemistry 10*, 4263−4270.
19. Rosenberg, R. C., Root, C. A., Wang, R., Cerdonio, M., and Gray, H. B. (1973) *Proc. Natl. Acad. Sci. U.S.A. 70*, 161−163.
20. Carlin, R. L. (1965) in *Transition Metal Chemistry* (Carlin, R. L., Ed.) Vol. 1, pp 1−32, Marcel Dekker, New York.
21. Rosenberg, R. C., Root, C. A., and Gray, H. B. (1975) *J. Am. Chem. Soc. 97*, 21−26.
22. Holmquist, B., Kaden, T. A., and Vallee, B. L. (1975) *Biochemistry 14*, 1454−1461.

BI9928952